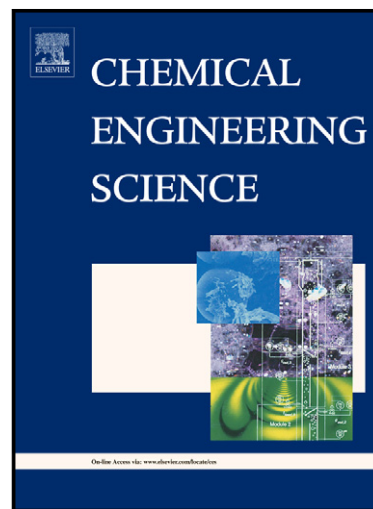


Author's Accepted Manuscript

A simple model for predicting the pressure drop and film thickness of non-Newtonian annular flows in horizontal pipes

Haiwang Li, Teck Neng Wong, Martin Skote, Fei Duan



PII: S0009-2509(13)00539-3
DOI: <http://dx.doi.org/10.1016/j.ces.2013.07.046>
Reference: CES11216

To appear in: *Chemical Engineering Science*

Received date: 19 March 2013
Revised date: 7 June 2013
Accepted date: 28 July 2013

Cite this article as: Haiwang Li, Teck Neng Wong, Martin Skote, Fei Duan, A simple model for predicting the pressure drop and film thickness of non-Newtonian annular flows in horizontal pipes, *Chemical Engineering Science*, <http://dx.doi.org/10.1016/j.ces.2013.07.046>

This is a PDF file of an unedited manuscript that has been accepted for publication. As a service to our customers we are providing this early version of the manuscript. The manuscript will undergo copyediting, typesetting, and review of the resulting galley proof before it is published in its final citable form. Please note that during the production process errors may be discovered which could affect the content, and all legal disclaimers that apply to the journal pertain.

1 **A simple model for predicting the pressure drop and film thickness of non-Newtonian**
2 **annular flows in horizontal pipes**

3
4 **Haiwang Li^{1,2}, Teck Neng Wong^{1,*}, Martin Skote¹, Fei Duan¹**

5
6 ¹School of Mechanical and Aerospace Engineering, Nanyang Technological University
7 50 Nanyang, Avenue, Singapore 639798,

8 ²National Key Lab. of Science and Technology on Aero-Engines, Beijing University of
9 Aeronautics and Astronautics,
10 Beijing, 100191, China

11 *Corresponding author. E-mail: mtnwong@ntu.edu.sg
12

13 **Abstract**

14 A model of two-phase non-Newtonian horizontal annular flows, which predicts film
15 thickness and pressure gradient from flowrates only, is presented. In the model, the gas and
16 non-Newtonian liquid flows are calculated separately based on the independent governing
17 equations. The shear stress balance at the gas-liquid interface is calculated in order to link
18 two phases together. The non-Newtonian fluid is assumed as a power-law shear-thinning
19 liquid. The logarithmic velocity distribution is chosen to calculate the turbulent velocity
20 profile in the gas core. The influences of entrainment and aeration are included in the model.
21 The pressure drop, film thickness, void fraction, the frictional multiplier, and
22 Lockhart-Martinelli parameter are predicted. The analytical model is compared with the
23 published experimental investigations, and the results show that the model can predict the
24 film thickness and pressure gradient simultaneously based on the flowrates of liquid and gas.
25 The frictional multiplier and Lockhart-Martinelli parameter are calculated at the same time,
26 and the predicted values are comparable with the experimental data. The difference between
27 the analytical model and the experiments is lower than 10%.

28
29 **Keywords:** Fluid Mechanics, Mathematical modeling, Multiphase flow, Non-Newtonian
30 fluids, Annular, entrainment

31 **Introduction**

32 In the recent years, considerable effort has been made to study simultaneous gas-liquid

1 flows in horizontal and inclined pipes (Al-Kizwini et al., 2013; Okawa et al., 2010; Tai and
2 Chung, 2010; Wang et al., 2012). The two-phase flows are commonly found in power plants,
3 chemical processes, nuclear reactors, and petroleum related industries. The three most
4 important hydrodynamic features of gas-liquid flows in engineering applications, including
5 the flow pattern, the void fraction, and the pressure drop of two-phase flows, have been
6 studied experimentally and theoretically (Al-Kizwini et al., 2013; Al-Sarkhi et al., 2012;
7 Baniamerian et al., 2012; Cioncolini and Thome, 2012; Okawa et al., 2010; Ren et al., 2012;
8 Tai and Chung, 2010; Wang et al., 2012; Xiao et al., 2011). An annular flow, which occurs at
9 relatively high gas flowrates, is defined with a gas core in the center of the channel and an
10 annular liquid film adjacent to the channel wall. With wide applications can be found in the
11 process industries (Srivastava, 1977), the annular flow has been investigated experimentally
12 (Al-Kizwini et al., 2013; Ashwood, 2010; Brill and Beggs, 1978; G. F. Hewitt, 1969;
13 Lockhart and Martinelli, 1949; Ren et al., 2012) and numerically (Rodriguez, 2009; Tai and
14 Chung, 2010).

15 Prediction of pressure loss and void fraction of annular flow is important for the accurate
16 design and optimization of multi-phase flows systems, as evidenced by the engineering
17 model development in decades (Ashwood, 2010; Cioncolini and Thome, 2012; Xiao et al.,
18 2011). The annular flow is traditionally analyzed through the triangular relationship (G. F.
19 Hewitt, 1969). Modeling of the annular flow can be generally broken into two physical
20 concepts. The first model, derived by the Ref (Owen and Hewitt, 1987), is a single-zone one
21 which describes the film without distinction between the wall and free wavy interface. As
22 originally presented, this model yields an estimate average film thickness and pressure loss
23 according to the entrainment data. Hurlburt and co-worker (Hurlburt, 2006; Schubring, 2009;
24 Wallis, 1969) developed another model, in which the waves and the base film were modeled
25 separately. Following the concept of Hurlburt, the effect of entrained fraction is added to
26 compute the local interfacial shear. The effects of base-wave division, coupling film and
27 entrainment behavior were considered in the model of Hurlburt (Hurlburt, 2006). Schubring
28 and co-worker (Schubring and Shedd, 2008, 2009a, b, 2011) developed the models which

1 include effects of wave magnitude, wave intermittency, and the sharp transitions between
2 base film and disturbance waves. However, the previous research efforts have been heavily
3 directed toward the two-phase flow of gas and Newtonian liquid, despite the increasing
4 industrial importance of non-Newtonian liquids, such as aeration of Newtonian broths in
5 biochemical reactors, continuous polymerization, transport of such non-Newtonian liquid
6 materials as drilling mud, greases, slurries, polymer solutions, etc. Limited information is
7 available for the case when the liquid phase is non-Newtonian flow. Therefore, it needs to
8 understand the annular flow behavior of non-Newtonian two-phase flow.

9 As an annular flow is often understood through triangular relationship, the empirical
10 relationship among film thickness, pressure drop, and flowrates (Srivastava and
11 Narasimhamurty, 1973; Tyagi and Srivastava, 1976; Xu et al., 2007) has been previously
12 analyzed. Srivastava and his co-worker (Srivastava, 1977; Tyagi and Srivastava, 1976)
13 proposed a non-Newtonian liquid-gas annular flow model to predict liquid holdup and
14 two-phase pressure drop. The logarithmic velocity distribution of turbulent flow was used to
15 predict the velocity distribution of the gas core. The previous work (Eisenberg and
16 Weinberger, 1979) measured the pressure drop and void fraction of two-phase
17 non-Newtonian flows; the measured results were compared with the model prediction which
18 was a modified version of the two-phase Newtonian flow. As a PhD student, Shu extended
19 the Newtonian model to the non-Newtonian two-phase flow model based on the relationship
20 of properties between Newtonian and non-Newtonian fluids (Shu, 1981). These models are
21 developed using the concept of triangular relationship of the annular flow. In order to
22 calculate one parameter, i.e. film thickness, the other parameters of flowrates and pressure
23 drop should be known. The application of models are limited because the values of film
24 thickness and pressure drop of a two-phase flow are difficult to be measured (Ashwood,
25 2010).

26 In summary, most of the previous modeling works have focused on the Newtonian flow,
27 and either pressure gradient or film thickness needs to be known although they are very
28 difficult to measure. In addition, the effects of aeration and entrainment were ignored in most

1 of studies. The model presented here improves these deficiencies. This paper develops a
2 model to predict the pressure drop and film thickness of a two-phase non-Newtonian
3 horizontal annular flow; the effects of entrainment and aeration are taken into account into
4 the model. The pressure drop, film thickness, void fraction, the frictional multiplier, and
5 Lockhart-Martinelli parameter are obtained using this model. These analytical results are
6 compared with the published experimental data (Schubring and Shedd, 2009a; Shu, 1981).

7 The paper is organized as follows: in section 2, the mathematical model is derived based
8 on the assumption of the logarithmic velocity distribution in the gas core. The results and
9 discussion are presented in section 3. The relationship among the void fraction, the frictional
10 multiplier, and Lockhart-Martinelli parameter are presented. The conclusions from the model
11 are presented in section 4.

12 13 **2. Mathematical model**

14 Figure 1 shows the model of a two-phase annular flow including the effects of
15 entrainment and aeration. In the annular flow, there exists an interface between the liquid film
16 and the gas core. In practice this vapor-liquid interface is covered by a complex pattern of
17 waves. The liquid in the form of small droplets, and the gas as small bubbles, are entrained
18 into the gas core and the liquid film, respectively, through the interfaces. However, for the
19 theoretical analysis, a model of the flow conditions is conceived and shown in Fig. 1 with the
20 following assumptions (Eisenberg and Weinberger, 1979; Shedd and Newell, 2004; Shu, 1981;
21 Srivastava, 1977):

- 22 (1) The flow in liquid film is laminar while the flow in gas core is turbulent.
- 23 (2) The liquid film is assumed symmetrical.
- 24 (3) The liquid film and the gas core have the same pressure gradient along flow
25 direction.
- 26 (4) Zero pressure gradients exist in the radial direction.
- 27 (5) The gas velocity is the sum of the interfacial velocity and the turbulent component.
- 28 (6) The interface between the liquid film and gas core is smooth.
- 29 (7) There is no velocity slip either between liquid and the tube wall or between liquid

1 and gas.

2 (8) The gravitational and acceleration efforts can be ignored in the both liquid and gas
3 phases.

4 (9) Densities of gas and non-Newtonian liquid are constant.

5 This model proceeds through the following steps:

6 (i) The flowrate of liquid film and gas core are obtained firstly;

7 (ii) The film thickness is estimated under the constant flowrates of gas and liquid;

8 (iii) The pressure drop in the two-phase flow is calculated according to the flowrates
9 and film thickness;

10 (iv) The single-phase pressure drop is established;

11 (v) The multiplier (ϕ_L) and Lockhart-Martinelli parameter (X) are established
12 according to single-phase and two-phase pressure drop.

13

14 2.1. Governing equation of liquid film

15 The momentum equation in the cylindrical coordinates can be described as (G. F. Hewitt,
16 1969; Shu, 1981)

$$17 \quad -\frac{\partial P}{\partial z} + \frac{1}{r} \frac{\partial}{\partial r} (r \bar{\tau}_{rz}) = 0 \quad (1)$$

18 where r and z are the radial and axial directions of cylindrical coordinates, and $\bar{\tau}$ is the
19 average value of shear stress. This equation is also the force balance of liquid and gas. The
20 first term is the pressure gradient, and the second term is the shear stress. In Eq.(1), the
21 viscous stress τ can be described as

$$22 \quad \tau = m \left(\frac{\partial u}{\partial r} \right)^n \quad (2)$$

23 for the power-law model. In the two-phase flow, m is called flow consistency index and n is
24 denoted as flow behavior index. The fluid is shear thinning for $n < 1$, and shear thickening
25 flow for $n > 1$. Noted that a Newtonian liquid can be considered to be a power-law liquid
26 with an exponent $n = 1$. The viscosity of liquid film can be described as (Wallis, 1969)

$$\mu_f = \alpha_f \mu_G + (1 - \alpha_f) \mu_L \quad (3)$$

where μ_f is the viscosity of liquid film, α_f is the fraction of aeration in liquid film, μ_G is the viscosity of pure gas, and μ_L is the viscosity of pure liquid. In general case, μ_G is small compared to the liquid viscosity μ_L , $\mu_G \ll \mu_L$, and hence Eq. (3) reduces to $\mu_f = (1 - \alpha_f) \mu_L$. Therefore, Eq. (1) can be formulated as:

$$-\left[\frac{dP}{dz}\right]_{t\phi} + \frac{1}{r} \frac{\partial}{\partial r} \left(r \cdot (1 - \alpha_f) m \cdot \left(\frac{\partial u}{\partial r} \right)^n \right) = 0 \quad (4)$$

Equation (4) describes the relationship between the pressure gradient and velocity profile. In this equation, the subscript of $t\phi$ means two-phase. From Eq. (4), the velocity profile of liquid film can be derived as:

$$u = A + \left\{ -\frac{1}{2(1 - \alpha_f) m} \cdot \left[\frac{dP}{dz} \right]_{t\phi} \right\}^{1/n} \cdot \left(\frac{1}{\frac{1}{n} + 1} \cdot r^{\frac{1}{n} + 1} + B \right) \quad (5)$$

where A and B are real number introduced by integration, defined according to the boundary conditions.

2.2 Boundary conditions of liquid film

The no-slip boundary condition at the wall is used

$$u_f = 0 \text{ at } r = R_t \quad (6)$$

where R_t is the radius of the tube. The other boundary condition is the velocity at the interface $r = R_i$, where R_i is the radius of the interface. From the force balance at the interface, the relationship between shear stress and pressure gradient can be described as

$$\bar{\tau}_{rz} \cdot 2\pi R_i = \left(-\frac{dP}{dz} \right)_{t\phi} \cdot \pi R_i^2 \quad (7)$$

where the subscript of r and z indicated r and z direction, and the shear stress $\bar{\tau}_{rz}$ can be written as

$$\bar{\tau}_{rz} = (1 - \alpha_f) m \cdot \left(\frac{\partial u_f}{\partial r} \right)^n \quad (8)$$

2 According to Eqs. (7) and (8), the boundary condition for the velocity at the interface can be
3 expressed as

$$u_f = C + R_i^{(1+n)/n} \cdot \left(-\frac{1}{2(1-\alpha_f)m} \cdot \left(\frac{dP}{dz} \right)_{i\phi} \right)^{1/n} \quad (9)$$

5 where C is the real number due to integration.

6

7

8 **2.3 Velocity profile of liquid film**

9 Substituting the boundary conditions described by Eqs. (6) and (9) into Eq. (5), the
10 velocity of liquid film can be written as

$$u_f = \left(\frac{1}{2m(1-\alpha_f)} \cdot \left(-\frac{dP}{dz} \right)_{i\phi} \right)^{\frac{1}{n}} \cdot \frac{n}{n+1} \cdot \left(R_i^{\frac{n+1}{n}} - r^{\frac{n+1}{n}} \right) \quad (10)$$

12

13 **2.4 Velocity profile of gas core**

14 The universal velocity profile is given in the form of three expressions for three regions;
15 the viscous sub-layer, the buffer layer and the inertial layer. These three sections can be found
16 in the previous study (Srivastava, 1977). The velocity distribution in the inertial layer of
17 single-phase flow can be described by a logarithmic profile as (Tyagi and Srivastava, 1976) :

$$\frac{u_{tur}}{u_\tau} = 2.5 \ln \left(\frac{ru_\tau}{\nu} \right) + 5.5 \quad (11)$$

19 where u_{tur} is the velocity of turbulent component along z direction, u_τ is the friction
20 velocity, and ν is the kinematic viscosity of the gas core. The velocity of gas core in a
21 two-phase flow can be divided into two parts (Srivastava, 1977; Tyagi and Srivastava, 1976)

$$u = u_i + u_{tur} \quad (12)$$

23 where u_i is the velocity of interface which can be calculated according Eq. (10). Following

24 the previous work, the friction velocity of u_τ is defined as $u_\tau = \sqrt{\tau_i / \rho_c}$ where τ_i is the

1 interfacial shear stress and ρ_c is the density of the gas core. The interfacial shear stress is
 2 defined as (Taitel and Dukler, 1976)

$$3 \quad \tau_i = f_i \cdot \frac{\rho_c \cdot (\bar{u}_c - u_i)^2}{2} \quad (13)$$

4 where f_i is the friction factor of interface, and \bar{u}_c is the average velocity of the gas core.
 5 Because of $\bar{u}_c \gg u_i$ and $f_i = f_c$ (Gazley, 1949) (f_c is the friction factor of gas core at the
 6 wall), Eq. (13) can be simplified into

$$7 \quad \tau_i = f_c \cdot \frac{\rho_c \bar{u}_c^2}{2} \quad (14)$$

8 In Eq. (14), f_c can be calculated using the suggested method of Taitel and Dukler (Taitel
 9 and Dukler, 1976):

$$10 \quad f_c = C_c \cdot \left(\frac{D_c \bar{u}_c}{\nu_c} \right)^{-a} \quad (15)$$

11 where the subscript of c means gas core, C_c is a coefficient (Taitel and Dukler, 1976) with a
 12 value of 0.046 for the turbulent flow. D_c is the hydraulic diameter, a is an index which is
 13 $a = 0.2$ in the turbulent flow, and ν_c is the kinematic viscosity of the gas core. The
 14 previous work (Agrawal et al., 1973) suggested that D_c can be calculated with the following
 15 expression

$$16 \quad D_c = \frac{4A_c}{S_c} = 2R_i \quad (16)$$

17 where A_c is the cross-sectional area of gas core and S_c is the perimeter of gas core. In Eq.
 18 (15), the kinematic viscosity can be described as

$$19 \quad \nu_c = \frac{\mu_c}{\rho_c} \quad (17)$$

20 where μ_c is the dynamic viscosity of gas core and ρ_c is the density of gas core. From

1 Landel's work (Landel, 1963), the viscosity of the non-Newtonian gas core can be expressed
2 with

$$3 \quad \mu_c = \mu_G \cdot (1-q)^{-2.5} \quad (18)$$

4 where μ_G is the dynamic viscosity and q is the volume fraction of liquid entrained into the
5 gas core. The density of the gas core is related to the flowrates of gas and fluid through:

$$6 \quad \rho_c = (1-q)\rho_G + q \cdot \rho_L \quad (19)$$

7 The subscript of G and L refer to gas and liquid respectively. Combining Eqs. (17), (18) and
8 (19), yields the kinematic viscosity of gas core:

$$9 \quad \nu_c = \frac{\mu_G \cdot (1-q)^{-2.5}}{(1-q)\rho_G + q \cdot \rho_L} \quad (20)$$

10 The relationship between gas flowrate Q_G and gas core flowrate Q_c is

$$11 \quad Q_c = \frac{(1-\alpha_f)}{(1-q)} \cdot Q_G \quad (21)$$

12 The average velocity of gas core is defined according to Eq. (21)

$$13 \quad \bar{u}_c = \frac{(1-\alpha_f)}{(1-q)} \cdot \frac{Q_G}{\pi R_i^2} \quad (22)$$

14 Substituting Eqs. (15), (20) and (22) into Eq. (14), the interfacial shear stress can be
15 described as

$$16 \quad \tau_i = C_c \cdot \left(\frac{2}{\nu_c} \cdot \frac{(1-\alpha_f)}{(1-q)} \cdot \frac{Q_G}{\pi} \right)^{-a} \cdot \frac{[(1-q)\rho_G + q \cdot \rho_L]}{2} \cdot \left[\frac{(1-\alpha_f)}{(1-q)} \cdot \frac{Q_G}{\pi} \right]^2 \cdot R_i^{a-4} \quad (23)$$

17 From Eq. (23), the friction velocity can be described as

$$18 \quad u_\tau = \left\{ \frac{C_c \cdot \left(\frac{2}{\nu_c} \cdot \frac{(1-\alpha_f)}{(1-q)} \cdot \frac{Q_G}{\pi} \right)^{-a} \left[\frac{(1-\alpha_f)}{(1-q)} \cdot \frac{Q_G}{\pi} \right]^2}{2} \right\}^{\frac{1}{2}} \cdot R_i^{\frac{a-4}{2}} \quad (24)$$

19 Substituting Eqs. (10) and (11) into Eq. (12), the turbulent component of gas core can be

1 calculated with the following expression

$$2 \quad u_c = \left\{ \frac{1}{2m(1-\alpha_f)} \cdot \left[-\frac{dP}{dz} \right]_{r\phi} \right\}^{\frac{1}{n}} \cdot \frac{n}{n+1} \cdot \left(R_i^{\frac{n+1}{n}} - R_i^{\frac{n+1}{n}} \right) + 2.5u_\tau \ln \left(\frac{ru_\tau}{V_c} \right) + 5.5u_\tau \quad (25)$$

3

4 **2.5 Pressure drop**

5 Pressure drop can be calculated from the relationship between the flowrate of liquid film
6 and velocity profile. From Eq. (10), the velocity can be obtained and then inserted into the
7 expression:

$$8 \quad Q_f = \int_{R_i}^{R_o} 2\pi u r dr \quad (26)$$

9 where Q_f is the volumetric flowrate of the liquid film. Substituting the velocity profile of
10 the liquid film in Eq. (10) into Eq. (26), the flowrate Q_f is presented as follows

$$11 \quad Q_f = 2\pi \cdot \left\{ \frac{1}{2m(1-\alpha_f)} \cdot \left[-\frac{dP}{dz} \right]_{r\phi} \right\}^{\frac{1}{n}} \cdot \frac{n}{n+1} \cdot \left\{ R_i^{\frac{n+1}{n}} \cdot \left(\frac{R_o^2 - R_i^2}{2} \right) - \left(\frac{n}{3n+1} \right) \cdot \left[R_i^{\left(\frac{3n+1}{n} \right)} - R_i^{\left(\frac{3n+1}{n} \right)} \right] \right\} \quad (27)$$

12 The flowrate of liquid film can be calculated according to the flowrate of the liquid. The
13 relationship is shown as

$$14 \quad Q_f \cdot (1-\alpha_f) = Q_L \cdot (1-q) \quad (28)$$

15 where Q_L is the total volumetric flowrate of the liquid. From Eqs. (27) and (28), the
16 pressure drop can be calculated according to the volumetric flowrate of the liquid

$$17 \quad \left[-\frac{dP}{dz} \right]_{r\phi} = \frac{2}{R_i} \cdot (1-\alpha_f) \cdot m \cdot \left\{ \frac{(1-q)}{(1-\alpha_f)} \cdot \frac{n+1}{n} \cdot F \cdot \left(\frac{Q_L}{\pi R_i^3} \right) \right\}^n \quad (29)$$

18 where F can be calculated as:

$$19 \quad F = \left\{ 1 - \left(\frac{R_i}{R_i} \right)^2 - \left(\frac{2n}{3n+1} \right) \cdot \left[1 - \left(\frac{R_i}{R_i} \right)^{\left(\frac{3n+1}{n} \right)} \right] \right\}^{-1} \quad (30)$$

20

1 **2. 6 The value of R_i**

2 The value of R_i is the critical parameter of the two-phase flow. The pressure and
 3 velocity can be calculated if the value of R_i is known. The gas core flowrate Q_c can be
 4 calculated from the velocity profile (Eq. (25))

$$5 \quad Q_c = \int_0^{R_i} 2\pi u_c r dr \quad (31)$$

6 From Eq.(21), the gas flowrate can be calculated as

$$7 \quad Q_G = H \cdot R_i^{\frac{a}{2}} \cdot \left[1.25 \ln \left(\frac{BR_i^{\frac{a-2}{2}}}{\nu} \right) + 2.125 \right] \quad (32)$$

$$8 \quad + I \cdot \left[\frac{2}{R_i} \cdot (1-\alpha_f) \cdot m \cdot \left\{ \frac{(1-q)}{(1-\alpha_f)} \cdot \frac{n+1}{n} \cdot F \cdot \left(\frac{Q_L}{\pi R_i^3} \right) \right\}^n \right]^{\frac{1}{n}} \cdot \left(R_i^2 \cdot R_i^{\frac{n+1}{n}} - R_i^{\frac{3n+1}{n}} \right)$$

8 where

$$9 \quad B = \left\{ \frac{C_c \cdot \left(\frac{2}{\nu_c} \cdot \frac{(1-\alpha_f)}{(1-q)} \cdot \frac{Q_G}{\pi} \right)^{-a} \left[\frac{(1-\alpha_f)}{(1-q)} \cdot \frac{Q_G}{\pi} \right]^2}{2} \right\}^{\frac{1}{2}} \quad (33)$$

$$10 \quad H = 2\pi \cdot \frac{(1-q)}{(1-\alpha_f)} \cdot \left\{ \frac{C_c \cdot \left(\frac{2}{\nu_c} \cdot \frac{(1-\alpha_f)}{(1-q)} \cdot \frac{Q_G}{\pi} \right)^{-a} \left[\frac{(1-\alpha_f)}{(1-q)} \cdot \frac{Q_G}{\pi} \right]^2}{2} \right\}^{\frac{1}{2}} \quad (34)$$

$$11 \quad I = \frac{\pi(1-q)}{(1-\alpha_f)} \cdot \left\{ \frac{1}{2m(1-\alpha_f)} \right\}^{\frac{1}{n}} \cdot \frac{n}{n+1} \quad (35)$$

12 Eq. (32) constitutes the relationship between Q_G , Q_L and R_i . When the value of Q_G
 13 and Q_L are known, the value of R_i can be calculated.

1

2 **2.7 Frictional multiplier, ϕ_L**

3 The liquid phase frictional multiplier ϕ_L is defined as follows (Lockhart and Martinelli,
4 1949)

$$5 \quad \phi_L = \left\{ \frac{\left[\left[\frac{dP}{dz} \right]_{i\phi} \right]^{\frac{1}{2}}}{\left[\left[\frac{dP}{dz} \right]_{spL} \right]} \right\} \quad (36)$$

6 For the single-phase flow of a power-law liquid, $\alpha_f = 0$, $R_i = 0$, $q = 0$, Eq. (29)
7 reduces into

$$8 \quad \left[\frac{dP}{dz} \right]_{spL} = \frac{2}{R_t} \cdot m \cdot \left\{ \frac{3n+1}{n} \cdot \left(\frac{Q_L}{\pi R_t^3} \right) \right\}^n \quad (37)$$

9 where the subscript of “ spL ” means single-phase liquid. When substituting Eqs. (29) and (37)
10 into Eq. (36), the multiplier can be expressed as

$$11 \quad \phi_L = (1 - \alpha_f)^{\frac{1}{2}} \cdot \left[\frac{(1-q)}{(1-\alpha_f)} \right]^{\frac{n}{2}} \cdot \left(\frac{n+1}{3n+1} \right)^{\frac{n}{2}} \cdot \left\{ 1 - \left(\frac{R_i}{R_t} \right)^2 - \left(\frac{2n}{3n+1} \right) \cdot \left[1 - \left(\frac{R_i}{R_t} \right)^{2\left(\frac{3n+1}{2n}\right)} \right] \right\}^{-\frac{n}{2}} \quad (38)$$

12

13 **2.8 The Lockhart-Martinelli parameter, X**

14 The Lockhart-Martinelli parameter X can be defined as (Lockhart and Martinelli, 1949)

$$15 \quad X = \left\{ \frac{\left[\left[\frac{dP}{dz} \right]_{spL} \right]^{\frac{1}{2}}}{\left[\left[\frac{dP}{dz} \right]_{spG} \right]} \right\} \quad (39)$$

16 This relationship is suitable for two-phase gas / Newtonian flow. For non-Newtonian flow,
17 some researchers (Eisenberg and Weinberger, 1979) defined a modified Lockhart-Martinelli
18 parameter X

$$X_{\text{mod}} = \left\{ \frac{\left[-\frac{dP}{dz} \right]_{\text{spL}}^{\text{mod}}}{\left[-\frac{dP}{dz} \right]_{\text{spG}}} \right\}^{\frac{1}{2}} \quad (40)$$

2 with

$$\left[-\frac{dP}{dz} \right]_{\text{spL}}^{\text{mod}} = \frac{\eta_{\text{wall-t}\phi}}{\eta_{\text{wall-spL}}} \cdot \left[-\frac{dP}{dz} \right]_{\text{spL}} \quad (41)$$

4 where $\eta_{\text{wall-t}\phi}$ and $\eta_{\text{wall-spL}}$ are the average apparent viscosity of the non-Newtonian liquid
5 (Eisenberg and Weinberger, 1979) in the case of annular flow and single-phase flow
6 respectively. The ratio between the two average apparent viscosities is:

$$\frac{\eta_{\text{wall-t}\phi}}{\eta_{\text{wall-spL}}} = \left\{ \frac{n+1}{(3n+1) \cdot \left[1-\alpha - \left(\frac{2n}{3n+1} \right) (1-\alpha)^{\frac{3n+1}{2n}} \right]} \right\}^{n-1} \quad (42)$$

8 with

$$\alpha = (1-q) \frac{R_i^2}{R_r^2} + (1-\alpha_f) \left(1 - \frac{R_i^2}{R_r^2} \right) \quad (43)$$

10 where α is the total void fraction of the two-phase flow. The single-phase gas pressure can
11 be calculated based on the force balance

$$2\pi R_i \tau_c = \left(-\frac{dP}{dz} \right)_{\text{spG}} \cdot \pi R_i^2 \quad (44)$$

13 From the expression of the shear stress of gas core in Eq.(23), the pressure drop of
14 single-phase gas is

$$\left[-\frac{dP}{dz} \right]_{\text{spG}} = \frac{C_c \rho_G Q_G^2 R_i^{a-5}}{\pi^2} \cdot \left(\frac{2\rho_G}{\mu_G} \cdot \frac{Q_G}{\pi} \right)^{-a} \quad (45)$$

16 Substituting Eqs. (41), (42) and Eq. (45) into the definition of X , the modified
17 Lockhart-Martinelli parameter X can be described as

$$X = \frac{\pi}{Q_G} \cdot \left(\frac{2m}{C_c \cdot \rho_G} \right)^{\frac{1}{2}} \cdot \left\{ \frac{n+1}{(3n+1) \cdot \left[1 - \alpha - \left(\frac{2n}{3n+1} \right) \left(1 - \alpha^{\frac{3n+1}{2n}} \right) \right]} \right\}^{\frac{n-1}{2}} \cdot \left\{ \frac{3n+1}{n} \cdot \left(\frac{Q_L}{\pi R_i^3} \right) \right\}^{\frac{n}{2}} \cdot \left(\frac{2\rho_G}{\mu_G} \cdot \frac{Q_G}{\pi} \right)^{\frac{a}{2}} \cdot R_i^{\frac{4-a}{2}} \quad (46)$$

The holdup of liquid, E_L , can be calculated as

$$E_L = \frac{\pi (R_i^2 - R_i^2) \cdot (1 - \alpha_f) + \pi R_i^2 \cdot q}{\pi R_i^2} \quad (47)$$

3. Results and Discussion

The mathematical model for the non-Newtonian fluid flow is compared with the published data from various sources (Ashwood, 2010; Brill and Beggs, 1978; Lockhart and Martinelli, 1949; Schubring and Shedd, 2009a; Taitel and Dukler, 1976). However, in the reported data, the volume fraction of liquid entrained and fraction of aeration in liquid film are unknown. Hence, in the present study, when the analytical model is compared with experimental data, the volume fraction of liquid entrained and the fraction of aeration of liquid film are set as zero. The analytical results are presented regarding the pressure drop of two-phase flow, the film thickness, the void fraction, the frictional multiplier, ϕ_l , and the Lockhart-Martinelli parameter, X .

3.1 Film thickness

The comparison between the analytical model and published experimental results is shown in Fig. 2. In the comparison, the average value of the measured thickness is used. The predicted film thickness is determined by Eq. (32). The flowrates of gas and liquid follow the information of previous experiments (Ashwood, 2010). The comparison shows that the analytical model can predict the film thickness within the error of $\pm 10\%$.

3.2 Liquid holdup

The aeration and entrainment phenomenon were shown in the visual experiments (Okawa et al., 2010; Ren et al., 2012). However there is inadequate experimental data about these effects. The values of the aeration and entrainment are assumed.

To validate the predict liquid holdup over a range of flow conditions, comparisons are

1 made with available experimental results published (Shu, 1981). Figure 3 presents
2 comparisons between the measured (symbols) and predicted (lines) average holdup variations
3 with the Lockhart-Martinelli parameter (X). In the calculation of Newtonian fluids ($n = 1$),
4 the aeration and entrainment are set to be $q = 0$ and $\alpha_f = 0$. The excellent agreement
5 shows that the effects aeration and entrainment is not significant for Newtonian flow. This
6 conclusion agrees well with the previous works. (Schubring and Shedd, 2009a; Shu, 1981).
7 The comparison of the predicted holdup for air–water experiments shows that the discrepancy
8 increases when viscosity of aqueous increases. As the liquid film viscosity increases, the
9 liquid film of aqueous can be highly aerated by small gas bubbles, hence the viscosity of
10 liquid film is lower than that of pure liquid. For the non-Newtonian flows (0.063 wt%
11 Separan, 0.125 wt% Separan, and 0.5 wt% Separan), the results show that the predicted
12 average holdup is higher than the measured values. The discrepancy increases with the
13 decrease of flow behavior index n due to the zero aeration and entrainment assumption.

14 In the experiments (Schubring and Shedd, 2009a), the actual degrees of aeration and
15 entrainment are unknown. Therefore the quantitative comparisons between analytical model
16 and experimental results are difficult to obtain. Figure 3 shows the results when the entrained
17 liquid fraction is $q = 0.05$ and void fraction is $\alpha_f = 0.05$. The model can predict the
18 observed trend of the experiments. The divergence between the model and the experimental
19 results can be improved by changing the values of aeration and entrainment.

20

21 3.3 Pressure gradient

22 Figure 4 compares the predicted pressure gradient and experimental results from Brill
23 and Beggs [2]. The experiments used various non-Newtonian fluids. The diameter of the pipe
24 is 0.01825 m. The flow behavior index changes from $n = 0.43$ to $n = 0.76$; the flow
25 consistency index changes from $m = 0.62 \times 10^{-3} \text{ N} \cdot \text{s}^n / \text{m}^2$ to $m = 40.3 \times 10^{-3} \text{ N} \cdot \text{s}^n / \text{m}^2$.
26 The superficial liquid Reynolds number (Re) ranges from 0.36 to 2,816. The gas Reynolds
27 number ranges from 1,339 to 45,727. The results show that the analytical model can predict

1 the measured pressure drop; the maximum difference between the model and the
 2 experimental results is 15%. The error increases as the index n decreases. According to the
 3 conclusion of Tyagi and Srivastava (Tyagi and Srivastava, 1976), the interface phenomenon
 4 becomes more complex as the decrease of the flow behavior index n . Due to the perturbation
 5 of pressure which leads to non-uniform radial pressure, and the pressures of two phases are
 6 unequal.

8 3.4 Frictional multiplier

9 Figure 5 presents comparisons between the measured (symbols) and predicted liquid
 10 phase frictional multiplier variations with the Lockhart-Martinelli parameter. The model
 11 agrees reasonable well with the experimental results. For a given value of the
 12 Lockhart-Martinelli parameter, decreasing the value of n gives a lower multiplier ϕ_L .
 13 Furthermore, the value of ϕ_L decreases with an increase of Lockhart-Martinelli parameter X .

14 3.5 Velocity profiles

15 Figures 6 (a) and (b) show velocity profiles of Newtonian and non-Newtonian annular
 16 flow in a horizontal pipe. The predicted velocity profile of air-water (Newtonian flow)
 17 annular flow is compared with the experiments (Ashwood, 2010). In the experiments, the
 18 diameter of the pipe is 0.0115 m, the gas flowrate is 0.01 m³/s, and the liquid flowrate is
 19 3.6×10^{-5} m³/s. The dimensionless distance and velocity are defined as follows

$$20 \quad \bar{R} = \frac{L}{D} \quad (48)$$

$$21 \quad \bar{U} = \frac{U}{U_{sg}} \quad (49)$$

22 where D is the diameter of the pipe and U_{sg} is the superficial gas velocity.

23 The gas core velocity profile varies relatively smooth except in the region of the
 24 vapor-liquid interface. In the most region of gas core, the velocity is uniform. The velocity
 25 varies sharply within the interfacial region as can be seen from Fig. 6(a).

26 Figure 6 (b) shows the velocity profile of the liquid film. The velocity exhibit a linear

1 behavior throughout their profiles which indicates that the entire film regions are dominated
2 by the viscous behavior. The model agrees well with the experiments (Kopplin, 2004). The
3 results also show that under the same flow conditions, the film thickness decreases whereas
4 the film velocity increases with decreasing index n . For the shear-thinning power-law liquid,
5 the shear stress decreases with the velocity gradient. The shear stress is reduced for lower
6 values of n . Under the same flowrate, the flow with lower n is faster and the thickness is
7 thinner. At the same time, the lower shear stress at the interface causes lower pressure loss
8 due to friction, and consequently the gas phase flows faster.

9 10 **4. Conclusions**

11 A method is introduced to predict the pressure drop and film thickness of a
12 non-Newtonian two-phase annular flow based on the flowrates of liquid and gas. In the
13 model, the non-Newtonian fluid is described using power-law liquid. The logarithmic
14 velocity distribution is chosen to describe the turbulent gas core velocity profile. The
15 influences of entrainment and aeration are included in the model.

16 The results show that the model can predict the film thickness and pressure drop. The
17 variation between the analytical model and the experimental results is lower than 10%. The
18 shear-thinning effect influences the flow behavior. Comparing with the Newtonian flow,
19 under the same flowrates, the non-Newtonian two-phase flow experiences a lower pressure
20 drop and the flow behavior is more complex. Under the same flowrates, the film thickness of
21 non-Newtonian flow is thinner.

22 23 **Acknowledgement**

24 The authors gratefully acknowledge research support from the Agency for Science,
25 Technology and Research (A*STAR) and Engineering Research Grant, SERC Grant No:
26 1021640147.

27 28 29 **References**

30 Agrawal, S.S., Gregory, G.A., Govier, G.W., 1973. An analysis of horizontal stratified

- 1 two-phase flow in pipes. *Canadian Journal of Chemical Engineering* 51, 280-286.
- 2 Al-Kizwini, M.A., Wylie, S.R., Al-Khafaji, D.A., Al-Shamma'a, A.I., 2013. The monitoring
3 of the two phase flow-annular flow type regime using microwave sensor technique.
4 *Measurement: Journal of the International Measurement Confederation* 46, 45-51.
- 5 Al-Sarkhi, A., Sarica, C., Qureshi, B., 2012. Modeling of droplet entrainment in co-current
6 annular two-phase flow: A new approach. *International Journal of Multiphase Flow* 39,
7 21-28.
- 8 Ashwood, A.C., 2010. Characterization of the macroscopic and microscopic mechanics in
9 vertical and horizontal annular flow, *Mechanical Engineering*. University of
10 Wisconsin-Madison.
- 11 Baniamerian, Z., Mehdipour, R., Aghanajafi, C., 2012. Analytical simulation of annular
12 two-phase flow considering the four involved mass transfers. *Journal of Fluids Engineering*,
13 *Transactions of the ASME* 134.
- 14 Brill, J.P., Beggs, H.D., 1978. *Two-phase Flow in Pipes*. The University of Tulsa, Tulsa, Okla.
- 15 Cioncolini, A., Thome, J.R., 2012. Void fraction prediction in annular two-phase flow.
16 *International Journal of Multiphase Flow* 43, 72-84.
- 17 Eisenberg, F.G., Weinberger, C.B., 1979. Annular two-phase flow of gases and
18 non-Newtonian liquids. *AIChE Journal* 25, 240-246.
- 19 G. F. Hewitt, N.S.H.T., 1969. *Annular Two-Phase Flow*. Pergamon Press,.
- 20 Gazley, C., 1949. *Interracial Shear and Stability in Two-phase Flow*. University of Delaware,
21 Newark.
- 22 Hurlburt, E.T., Fore, L.B., Bauer, R.C., 2006. A Two Zone Interfacial Shear Stress and Liquid
23 Film Velocity Model for Vertical Annular Two-Phase Flow, ASME 2006 2nd Joint
24 U.S.-European Fluids Engineering Summer Meeting Collocated With the 14th International
25 Conference on Nuclear Engineering (FEDSM2006) ASME, Miami, Florida, USA, pp.
26 677-684.
- 27 Kopplin, C.R., 2004. Local liquid velocity measurements in horizontal, annular two-phase
28 flow. University of Wisconsin-Madison, Madison, Wisconsin, USA.
- 29 Landel, R.F., B. G. Moser, A. J. Bauman, 1963. Proceedings of the Fourth International
30 Congress on Rheology, in: Copley, A.L. (Ed.), *Proceedings of the Fourth International*
31 *Congress on Rheology*. Brown University, New Yoke.
- 32 Lockhart, R.W., Martinelli, R.C., 1949. Proposed correlation of data for isothermal two-phase,
33 two-component flow in pipes. *Chemical Engineering Progress* 45, 39-48.
- 34 Okawa, T., Goto, T., Yamagoe, Y., 2010. Liquid film behavior in annular two-phase flow
35 under flow oscillation conditions. *International Journal of Heat and Mass Transfer* 53,
36 962-971.
- 37 Owen, D.G., Hewitt, G.F., 1987. An improved annular two-phase flow model.
- 38 Ren, S.J., Tan, C., Dong, F., 2012. Two phase flow visualization in an annular tube by an
39 electrical resistance tomography, pp. 488-492.
- 40 Rodriguez, J.M., 2009. Numerical simulation of two-phase annular flow. Rensselaer
41 Polytechnic Institute, New York.
- 42 Schubring, D., Shedd, T.A., 2008. Wave behavior in horizontal annular air-water flow.

- 1 International Journal of Multiphase Flow 34, 636-646.
- 2 Schubring, D., Shedd, T.A., 2009a. Critical friction factor modeling of horizontal annular
3 base film thickness. International Journal of Multiphase Flow 35, 389-397.
- 4 Schubring, D., Shedd, T.A., 2009b. Prediction of wall shear for horizontal annular air-water
5 flow. International Journal of Heat and Mass Transfer 52, 200-209.
- 6 Schubring, D., Shedd, T.A., 2011. A model for pressure loss, film thickness, and entrained
7 fraction for gas-liquid annular flow. International Journal of Heat and Fluid Flow 32,
8 730-739.
- 9 Schubring, D.L., 2009. Behavior interrelationships in annular flow. University of
10 Wisconsin-Madison, Madison, Wisconsin.
- 11 Shedd, T.A., Newell, T.A., 2004. Characteristics of the liquid film and pressure drop in
12 horizontal, annular, two-phase flow through round, square and triangular tubes. J. Fluids Eng.
13 126, 807-817.
- 14 Shu, M.T., 1981. Horizontal Two-phase Flow of Gases and Non-Newtonian Liquids. Drexel
15 University, Philadelphia, p. 271.
- 16 Srivastava, R.P.S., 1977. Liquid film thickness in annular flow. Chemical Engineering
17 Science 28, 819-824.
- 18 Srivastava, R.P.S., Narasimhamurty, G.S.R., 1973. Hydrodynamics of non-Newtonian
19 two-phase flow in pipes. Chemical Engineering Science 28, 553-558.
- 20 Tai, C.F., Chung, J.N., 2010. A direct numerical simulation of annular two-phase laminar
21 flow and heat transfer in a circular pipe. International Journal of Computational Methods in
22 Engineering Science and Mechanics 11, 230-246.
- 23 Taitel, Y., Dukler, A.E., 1976. A model for predicting flow regime transitions in horizontal
24 and near horizontal gas-liquid flow. AIChE Journal 22.
- 25 Tyagi, K.P., Srivastava, R.P.S., 1976. Flow behaviour of non-Newtonian liquid-air in annular
26 flow. The Chemical Engineering Journal 11, 147-152.
- 27 Wallis, G.B., 1969. One-dimensional two-phase flow. McGraw-Hill, New York.
- 28 Wang, R., Lee, B.A., Lee, J.S., Kim, K.Y., Kim, S., 2012. Analytical estimation of liquid film
29 thickness in two-phase annular flow using electrical resistance measurement. Applied
30 Mathematical Modelling 36, 2833-2840.
- 31 Xiao, R., Wei, B., Chen, G., Xun, H., 2011. The calculation on liquid holdup in horizontal
32 gasliquid two-phase annular flow, pp. 5362-5364.
- 33 Xu, J.y., Wu, Y.x., Shi, Z.h., Lao, L.y., Li, D.h., 2007. Studies on two-phase co-current
34 air/non-Newtonian shear-thinning fluid flows in inclined smooth pipes. International Journal
35 of Multiphase Flow 33, 948-969.

36
37
38
39
40

41 **List of figures**

42 Fig. 1 Model of annular flow with liquid entrainment into gas core and aeration in the liquid

1 film

2 Fig. 2 Comparison of the experimental film thickness with the analytical model

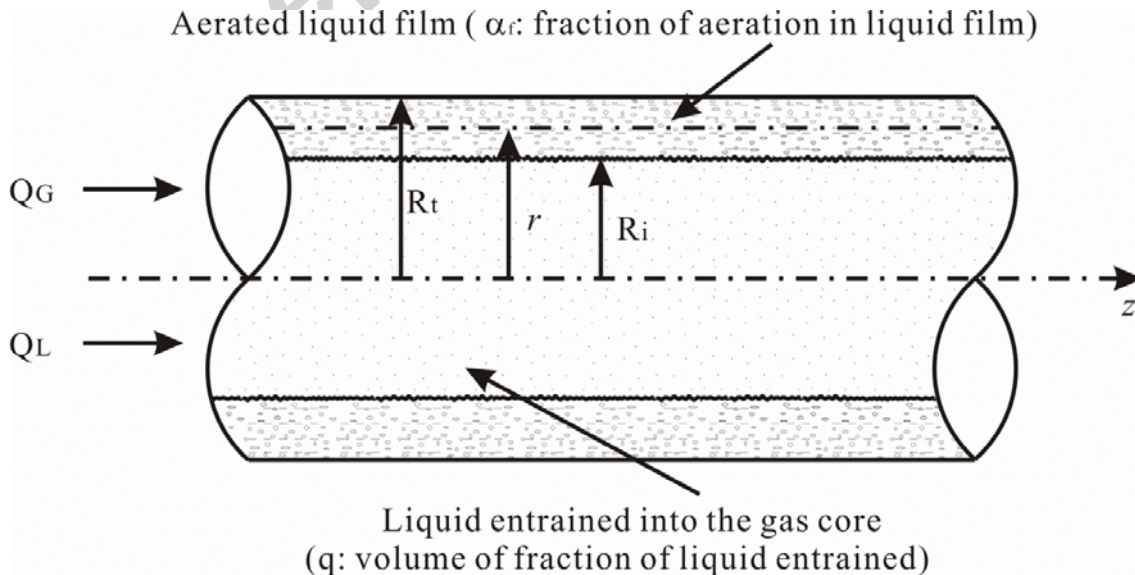
3 Fig. 3 Comparisons between the measured (symbols) and predicted (lines) average liquid
4 holdup with Lockhart-Martinelli parameter

5 Fig. 4 Comparison of the experimental pressure drop with the analytical model

6 Fig. 5 Comparisons between the measured (symbols) and predicted (lines) liquid phase
7 frictional multiplier with Lockhart-Martinelli parameter

8 Fig. 6 Comparison of the experimental velocity profile with the analytical model

9
10
11
12
13
14
15
16
17
18
19
20
21
22
23
24



25

1

2 Fig. 1 Model of annular flow with liquid entrainment into gas core and aeration in the liquid

3 film

4

5

6

7

8

9

10

11

12

13

14

15

16

17

18

19

20

21

22

23

24

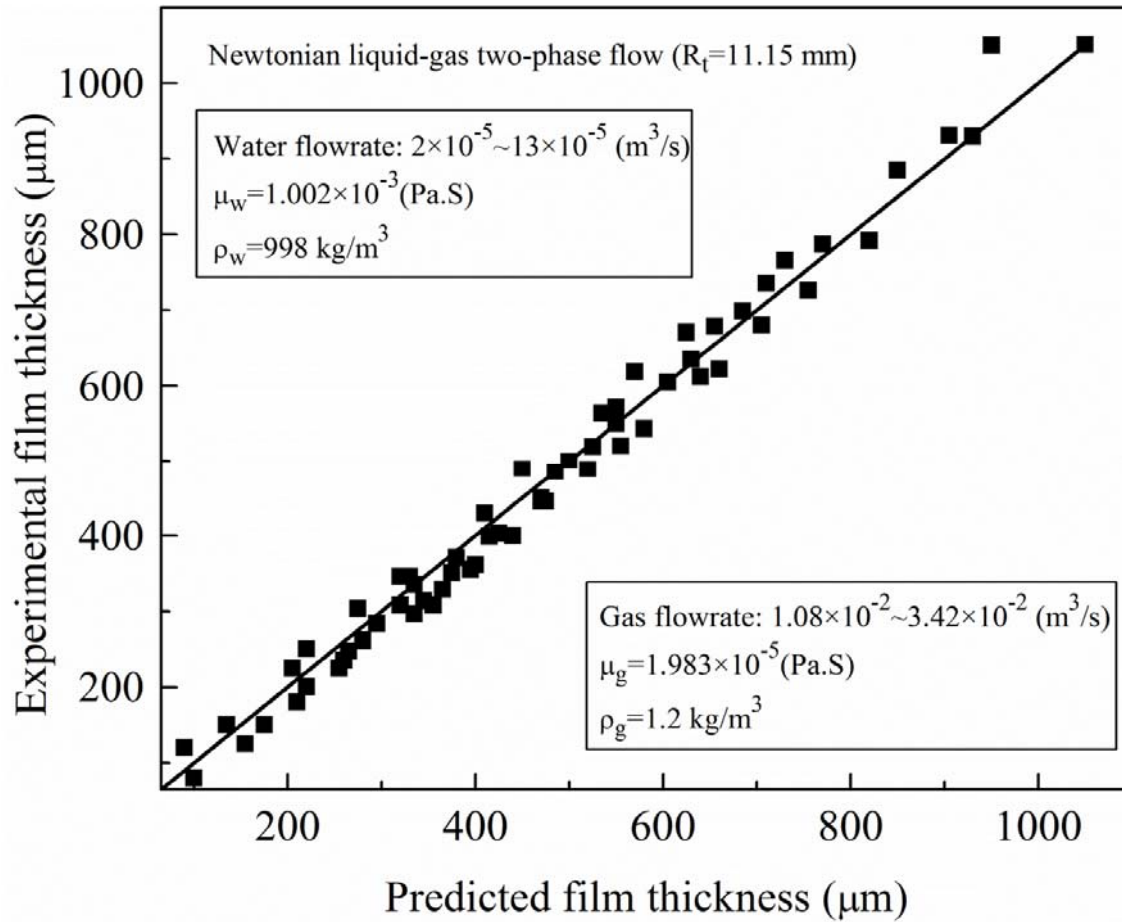
25

26

27

28

Accepted manuscript



1

2 Fig. 2 Comparison of the experimental film thickness (Ashwood, 2010) with the analytical
 3 model

4

5

6

7

8

9

10

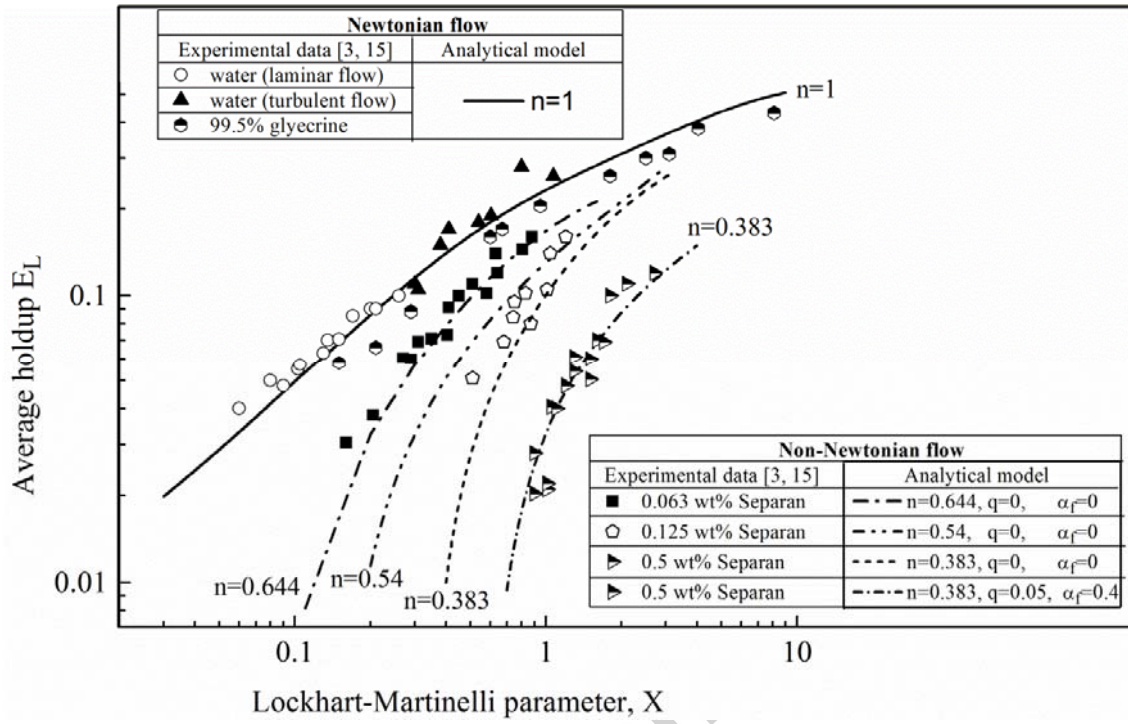
11

12

13

14

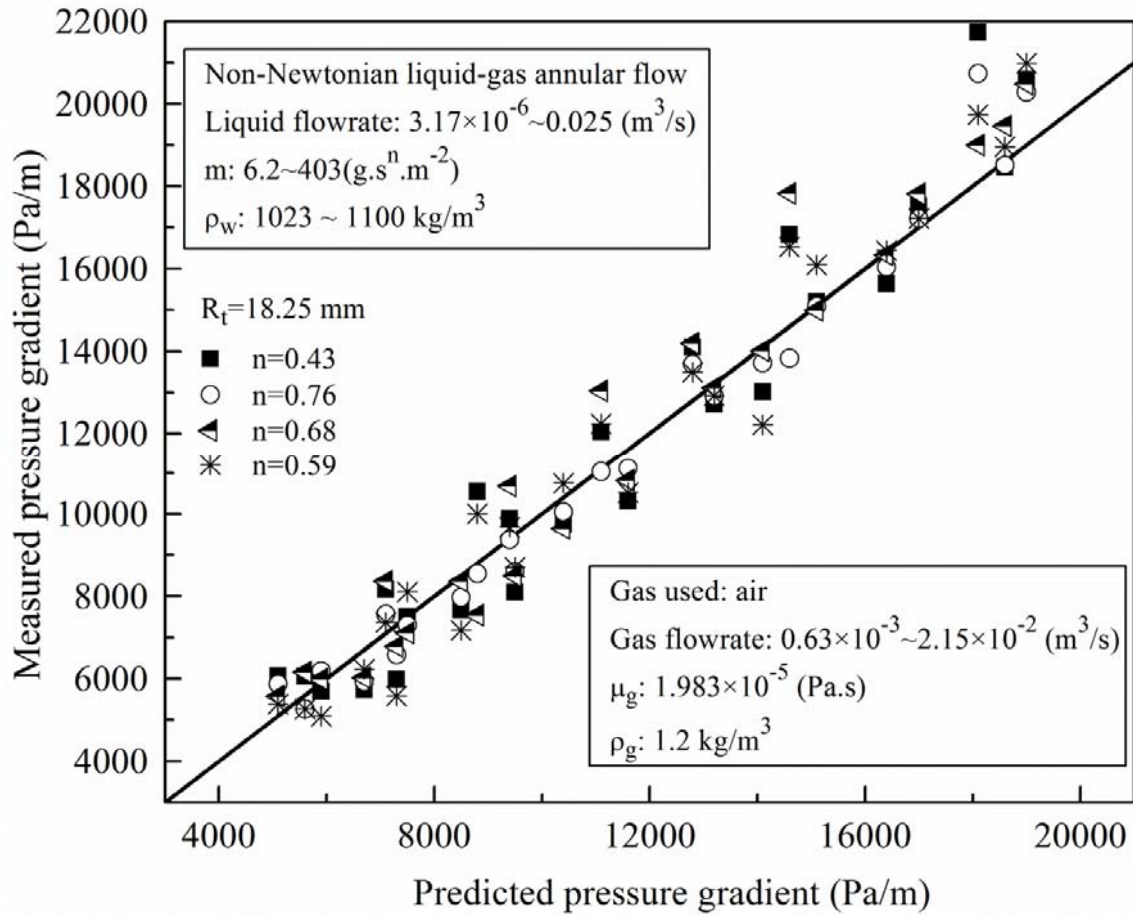
1



2

3 Fig. 3 Comparisons between the measured (symbols) and predicted (lines) average liquid
4 holdup with Lockhart-Martinelli parameter

5



1

2 Fig. 4 Comparison of the experimental pressure drop (Brill and Beggs, 1978) with the
 3 analytical model

4

5

6

7

8

9

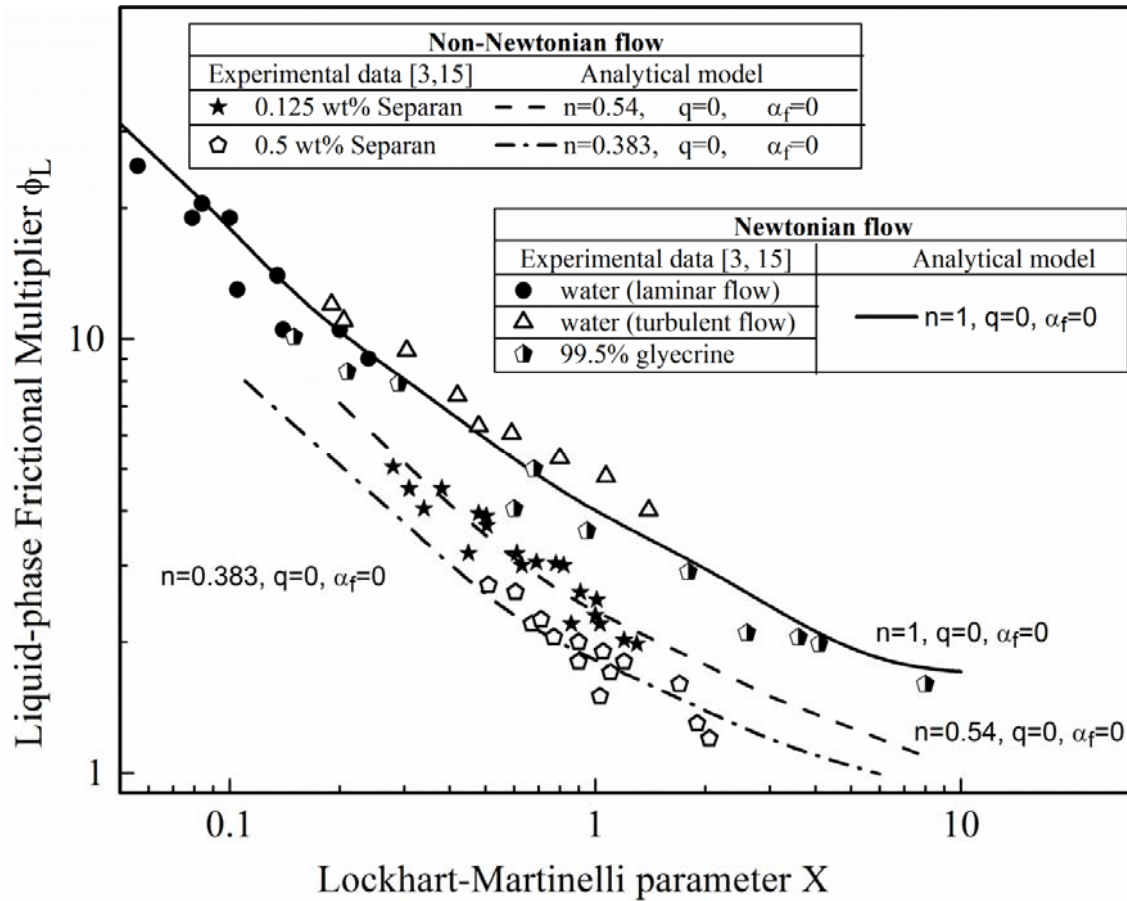
10

11

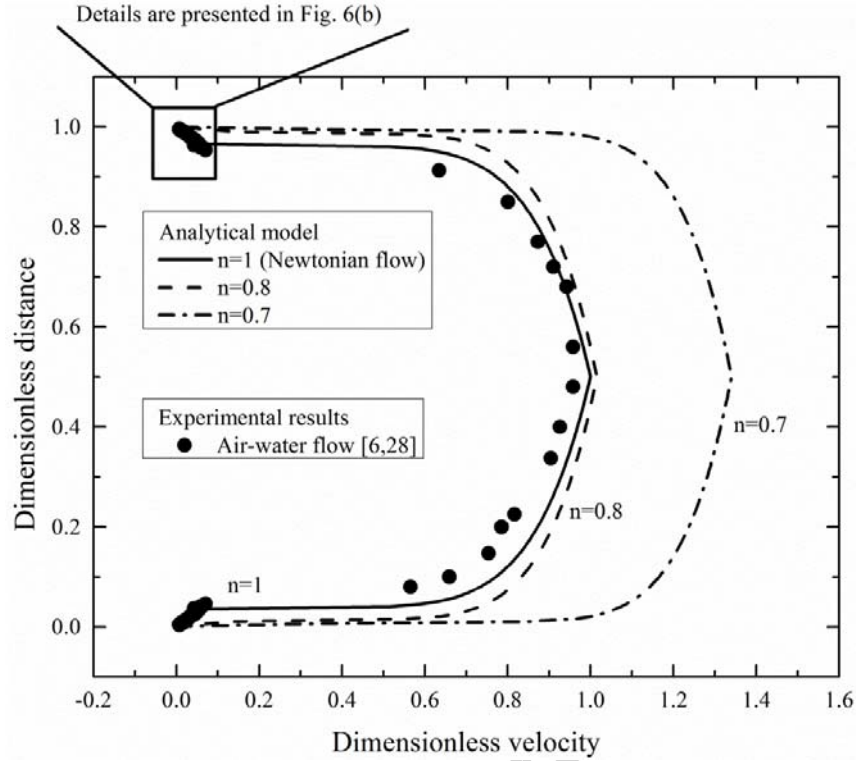
12

13

14



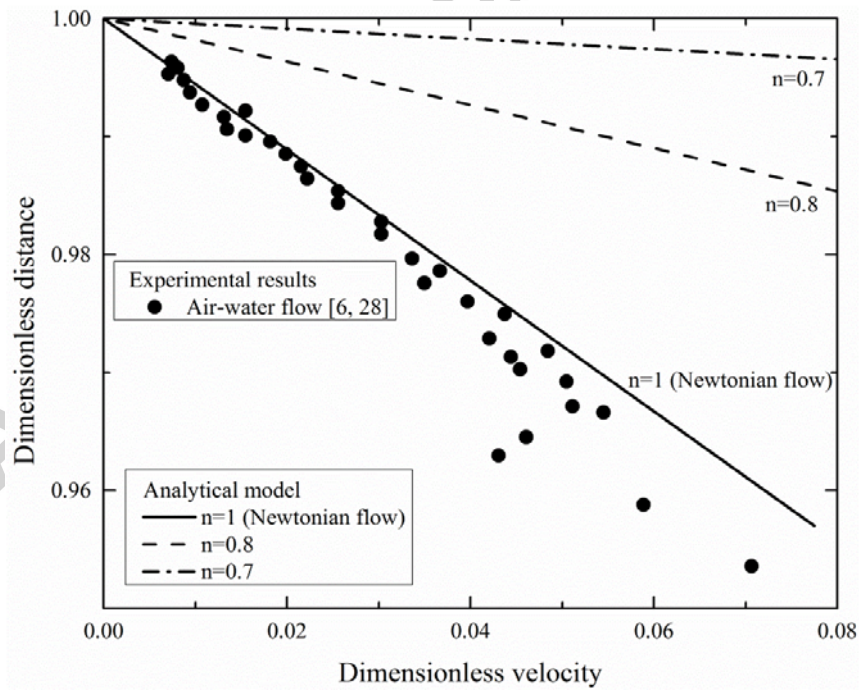
1
 2 Fig. 5 Comparisons between the measured (symbols) and predicted (lines) liquid phase
 3 frictional multiplier with Lockhart-Martinelli parameter
 4
 5
 6
 7
 8
 9
 10
 11
 12
 13
 14



1

2

(a) Velocity profiles of Newtonian and non-Newtonian annular flow



3

4

(b) Dimensionless liquid film velocity versus distance

5

Fig. 6 Comparison of the experimental velocity profile (Ashwood, 2010; Kopplin, 2004) with

6

the analytical model

1

2

3 Highlights

4 1. An analytical model to predict non-Newtonian liquid-gas annular flow.

5 2. This model predicts the film thickness and pressure gradient at the same time only based
6 on the flow rates of liquid and gas.

7 3. The influence of entrainment and aeration are predicted.

8 4. The difference between the model and the experimental results is lower than 10%.

Accepted manuscript